Molecules and fossils tell distinct yet complementary stories of mammal diversification

Highlights

d Mammal fossils show a Paleocene pulse of lineage turnover not found in the timetree

d Fossil- and timetree-based rates converge at the present showing unbiased tip rates

d Tip-level speciation rates are identifiable for studying present-day rate processes

d Clade-level distributions of tip speciation rates contain signals of past rate shifts

Authors

Nathan S. Upham, Jacob A. Esselstyn, Walter Jetz

Correspondence

nathan.upham@asu.edu (N.S.U.), walter.jetz@yale.edu (W.J.)

In brief

Upham et al.'s analysis of mammal speciation and extinction rates compares estimates derived from fossils and molecular timetrees. Fossils reconstruct a Paleocene speciation pulse that was erased by extinction and is thus undetectable from timetrees alone. Despite deep-time bias, timetrees offer unbiased snapshots of modern speciation processes.

Article

Molecules and fossils tell distinct yet complementary stories of mammal diversification

Nathan S. Upham,[1,2,3,5,6,*] Jacob A. Esselstyn,[4] and Walter Jetz[1,2,*]
[1]Department of Ecology & Evolutionary Biology, Yale University, New Haven, CT 06511, USA
[2]Center for Biodiversity and Global Change, Yale University, New Haven, CT 06511, USA
[3]School of Life Sciences, Arizona State University, Tempe, AZ 85287, USA
[4]Department of Biological Sciences and Museum of Natural Science, Louisiana State University, Baton Rouge, LA 70803, USA
[5]Twitter: @n8_upham
[6]Lead contact
*Correspondence: nathan.upham@asu.edu (N.S.U.), walter.jetz@yale.edu (W.J.)
https://doi.org/10.1016/j.cub.2021.07.012

SUMMARY

Reconstructing the tempo at which biodiversity arose is a fundamental goal of evolutionary biologists, yet the relative merits of evolutionary-rate estimates are debated based on whether they are derived from the fossil record or time-calibrated phylogenies (timetrees) of living species. Extinct lineages unsampled in timetrees are known to "pull" speciation rates downward, but the temporal scale at which this bias matters is unclear. To investigate this problem, we compare mammalian diversification-rate signatures in a credible set of molecular timetrees (n = 5,911 species, ~70% from DNA) to those in fossil genus durations (n = 5,320). We use fossil extinction rates to correct or "push" the timetree-based (pulled) speciation-rate estimates, finding a surge of speciation during the Paleocene (~66–56 million years ago, Ma) between the Cretaceous-Paleogene (K-Pg) boundary and the Paleocene-Eocene Thermal Maximum (PETM). However, about two-thirds of the K-Pg-to-PETM originating taxa did not leave modern descendants, indicating that this rate signature is likely undetectable from extant lineages alone. For groups without substantial fossil records, thankfully all is not lost. Pushed and pulled speciation rates converge starting ~10 Ma and are equal at the present day when recent evolutionary processes can be estimated without bias using species-specific "tip" rates of speciation. Clade-wide moments of tip rates also enable enriched inference, as the skewness of tip rates is shown to approximate a clade's extent of past diversification-rate shifts. Molecular timetrees need fossil-correction to address deep-time questions, but they are sufficient for shallower time questions where extinctions are fewer.

INTRODUCTION

The last 180 million-years of mammalian evolution have resulted in 6,400 living species[1,2] and many thousands of extinct taxa.[3,4] As one of the few large clades with ample paleo- and neontological evidence, mammals are a useful vehicle for investigating whether general patterns of evolutionary-rate variation are detectable through time.[5–7] However, even with abundant fossil[8] and genomic[9] resources, meaningfully integrating these data and their associated biases is challenging.[10–12] Deep-time questions, in which rate information among major "backbone-level" lineages is leveraged to test the biological impact of ancient earth-history events (e.g., Meredith et al.[13] and Oliveros et al.[14]), are at the limits of our capacity for inference from neontological data alone. That is because lineages are "erased" by extinctions with greater frequency as one moves back in time.[15] This temporal phenomenon causes rate underestimates from time-calibrated molecular phylogenies of living species alone (extant timetrees[16–18]). Further challenging inferences, fossils at older time intervals tend to be less abundant[3] and more spatially biased than more recent paleontological horizons.[19]

Thus, reconciling the respective biases of fossils and molecules at different timescales may help clarify when their respective insights are expected to be complementary versus confounding.

The limits of inferring diversification rates from extant timetrees were recently formalized by Louca and Pennell,[20] who found that, in the absence of additional fossil or demographic information, any given timetree may be equally explained by an infinite number of diversification scenarios. That is, speciation (λ) and extinction (m) rates are non-identifiable from timetrees alone; however, one class of rate parameters, referred to as "pulled" rates, does emerge as being identifiable: "pulled speciation rate" (λ_p), "pulled diversification rate" (r_p), and "sampling fraction 3 speciation rate at the instantaneous present" ($r\lambda_0$[20,21]). The pulling in this context represents how unsampled extinctions, especially at older time intervals, and incomplete modern sampling cause speciation-rate underestimation.[20] Indeed, several aspects of diversification tempo should still be estimable from extant timetrees and made more reliable by reference to parallel evidence sources such as fossils.[12,15,22–25]

Building on those insights, we suggest that the goal of empirical investigations into questions of deep-time evolutionary

history, at least for mammals and other fossil-rich clades, should be framed as a two-part endeavor: (1) leverage as much fossil information as possible for the time period(s) in question, and use that to exclude diversification scenarios that might be indistinguishable by molecular data alone (see also[15,26]); and (2) compare parametric estimates of species' birth and death (e.g., Morlon et al.[27] and Rabosky[28]) with metrics for pulled (l_p) and tip (l_0) speciation rates, since the latter two metrics should be identifiable when taxon sampling is known and thus instructive about the biases of the former. Making these comparisons in mammals should demonstrate the timescale at which molecular timetree-based inferences can be trusted. Unbiased estimation of "tip rates" of species-specific speciation, l_0, was previously demonstrated to require all extant taxa to be sampled or otherwise modeled (e.g., using the tip DR statistic[29,30]). However, in mammals, it has only recently become possible to estimate tip rates robustly, thanks to new species-level timetrees that model uncertainty in topology and node ages.[2] Speciation and extinction rates through time have not yet been characterized across these "backbone-and-patch" mammal trees,[2] nor have they been used to evaluate deep-time questions relative to previous supertree-based inferences (e.g., Bininda-Emonds et al.[31] and Purvis et al.[32]) or fossil mammal occurrences.[8]

Herein, we apply this two-part framework to investigate a key deep-time question in the radiation of mammals: did early mammals exhibit a burst of lineage diversification coincident with, well before, or well after the Cretaceous-Paleogene (K-Pg) boundary 66 million years ago (Ma)? These hypotheses are known as the Suppression,[33,34] Early Rise,[13] and Delayed Rise[31] models, respectively (reviewed in Grossnickle et al.[35] as relates to ecological diversification, but with implications for lineage diversification). The latter model of Delayed Rise emphasizes that recovery from the Paleocene-Eocene Thermal Maximum (PETM) ~56 Ma spurred more divergences within crown mammals than did the K-Pg mass extinction or earlier events.[31,36,37] Alternatively, the Early Rise model emphasizes that co-diversification with angiosperms in the late Cretaceous (85–75 Ma) impacted mammal radiations more than the K-Pg event.[13,35,38] These Mammalia-wide hypotheses overlap to some degree with Placentalia-specific models of Short/Long Fuse and Hard/Soft Explosive,[35,39,40] sparking confusion regarding the extent to which fossil-based conclusions (e.g., Grossnickle and Newham,[34] Wilson et al.,[38] and Pires et al.[41]) should be used to generate timetree-testable predictions for extant lineages. The K-Pg and PETM events both involved global climatic changes, the former by an extraterrestrial bolide impact and associated volcanism,[42] and the latter by a catastrophic release of carbon dioxide and subsequent 5°C to 8°C spike in temperatures.[37] Thus, we here use these climatic perturbations for testing (1) the extent to which inferences based on fossils, timetrees, or both combined illuminate the same or different aspects of mammalian evolutionary response, and (2) how the reliability of paleo- and neontological information sources varies from deep to shallow time.

Our specific objectives are 3-fold. First, we test for branch-specific rate shifts in the mammal timetrees relative to the K-Pg and PETM events to assess whether any residual impact signature has been retained in the branching times of extant lineages. Second, we directly compare diversification rates derived

from fossil genus durations versus timetrees, and reconcile their contrasting signals via the formation of a combined rate metric that "pushes" the pulled rates of speciation to correct their undersampling. Finally, we evaluate how the identifiable estimators of tip speciation rate and pulled speciation rate can be applied to assess clade-wise rate variation using timetrees alone. Overall, we show that while timetree-based rate estimates are highly uncertain at deep timescales, they are increasingly reliable closer to the present. Joining the timetree- and fossil-based inferences helps us narrow the range of possible diversification scenarios for mammals and, more broadly, to demonstrate that, even for clades without fossils, tip rates carry fairly reliable signatures of shallow-time evolutionary processes.

RESULTS

Broad tempo of diversification in the Mammalia timetree

The timetree of extant mammals shows that while the earliest divergences of crown Marsupialia and crown Placentalia occurred prior to the K-Pg boundary, and are thus consistent with the Early Rise model, the vast majority of intraordinal diversity arose after the PETM ~56 Ma (Figures 1 and 2A). The first 4 placental divergences unambiguously preceded the K-Pg event, as evidenced by divergence-time 95% highest posterior density (HPD) intervals that do not overlap 66 Ma (Figure 2A; filled circles). However, the next 29 placental divergences have 95% HPDs that overlap the K-Pg event, including the divergences of 12 superordinal lineages (Figure 2A, open circles), 9 crown orders (Figure 3A), and 8 intraordinal splits. In Marsupialia, the first 5 splits after the crown divergence overlap the K-Pg boundary, all at the superordinal level. Of those 34 divergences that overlap the K-Pg boundary, 18 also overlapped the PETM, making their timings statistically indistinguishable from causality by either event. The next 14 mammal divergences overlap the PETM exclusively, including crown ages of Paenungulata (Hyracoidea + Sirenia + Proboscidea), 4 orders (Lagomorpha, Artiodactyla, Monotremata, and Diprotodontia), and 9 intraordinal splits within bats and rodents (Table S1). Thus, the K-Pg and PETM events compare by having the possible coincidence of 34 versus 32 mammal divergences, respectively, of which 16 versus 14 are respectively exclusive to those events, providing timetree-based evidence for the Suppression and Delayed Rise models. By contrast, only 7 pre-K-Pg divergences of crown Theria support the Early Rise model using the extant timetree.

Branch-specific rate shifts in the extant timetree

Across 10 timetrees, BAMM estimates a tree-wide mean speciation rate of 0.206 (95% CI: 0.188–0.223) and mean extinction rate of 0.068 (0.053–0.088, units of species/lineage/Ma). The mean number of branch-specific shifts is 36.7 (95% CI for 10 runs: 27.9–43.4; Figure S1). A total of 253 shifts are detected in one or more trees, of which 208 are up-shifts (increases in net diversification rate) and 45 are down-shifts (Figures 3B and 4A). We identify 24 rate shifts that are consistently present in at least five of the 10 trees (Figures 1, 3B and 4A; Table S2), including 9 shifts paired (occurring on adjacent branches in different trees) and 18 non-nested shifts (Figure 1; see Supplemental Information for further summaries of the BAMM runs). Of those consistent shifts, we found substantial variation in the
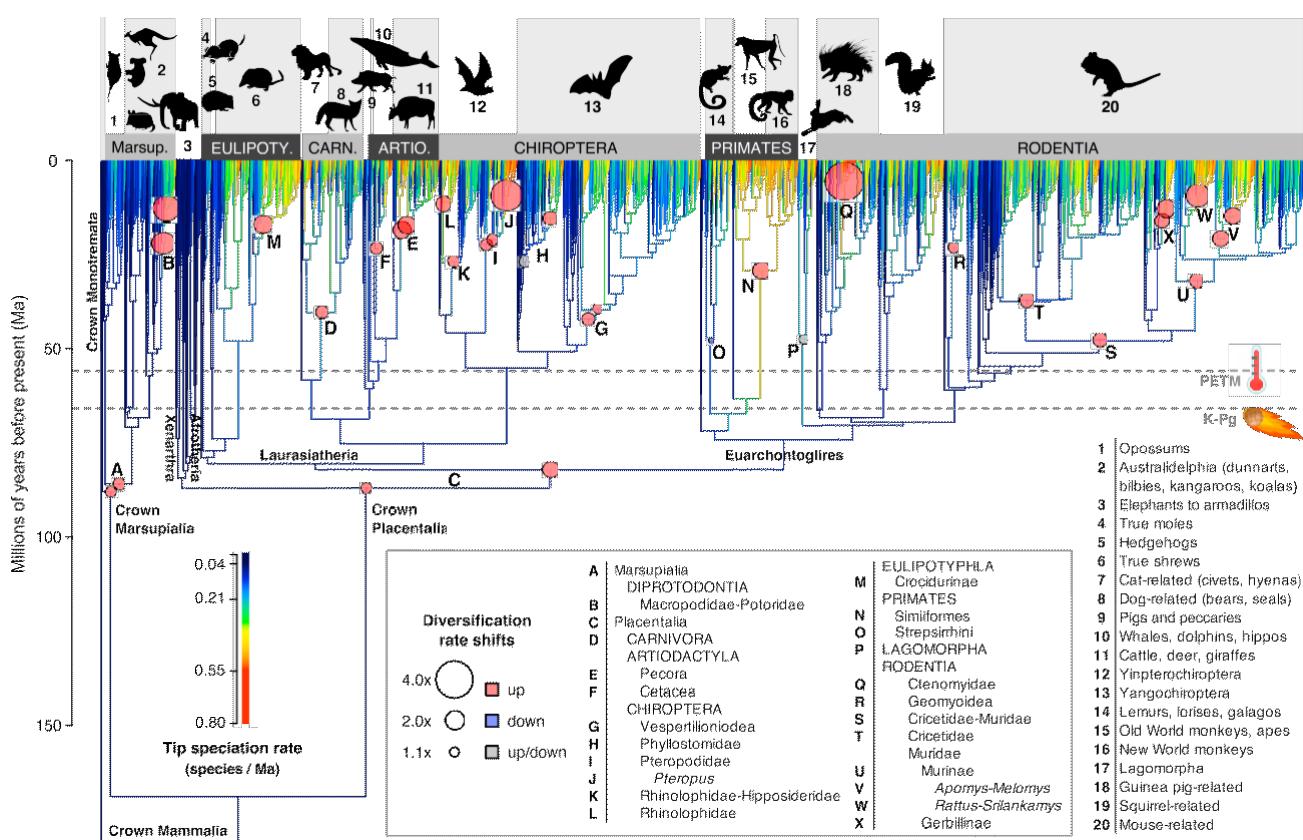
Figure 1. Extant time-calibrated molecular phylogeny for 5,911 species of mammals globally
The maximum clade credibility topology of 10,000 node-dated timetrees is shown with branches colored according to tip-level speciation rates (tip DR metric) and marked with 24 shifts in branch-specific net diversification rates inferred using BAMM (nodes A–X; shifts with multiple circles were inferred on either branch, not both, over a sampling of 10 trees from the credible set). Highlighted at 66 million years ago (Ma) is the extraterrestrial bolide impact that coincided with the Cretaceous-Paleogene (K-Pg) boundary, and at 56 Ma is the Paleocene-Eocene Thermal Maximum (PETM). Tip speciation rates are reconstructed to interior branches using Brownian motion for visualization purposes only. Numbered labels correspond to monophyletic groups listed in the plot periphery: Marsup., Marsupialia; Eulipoty., Eulipotyphla; Carn., Carnivora; Artio., Artiodactyla. Artwork is public domain from phylopic.org, open-source fonts, and creazilla.com (see Acknowledgments). See also Figure S1 and Table S2.

number of shifts per patch clade that was used to construct the backbone-and-patch mammal trees, indicating that the location of rate shifts was unrelated to patch clade delimitation (Figure S4).

In the case of the Placentalia and 8 other rate shifts, shift location is contingent on the rooting of the tree (see Upham et al.[2]) and how the concomitant background rate varies (Table S2), highlighting the relevance of considering a sample of phylogenies. Four of the 24 shifts are ever recorded as decreases, and only 1 shift is consistently a decrease across trees: the strepsirrhine primates (lemurs, lorises, and galagos, O), for which we show a 1.7-fold reduction in net diversification relative to the background rate (Figure 1; Table S2). Overall, the 20 consistent up-shifts have larger magnitudes nearer the present, with a 2.2-fold mean shift factor in the Miocene versus 1.3-fold in each the Oligocene and Eocene (Figure 4A; three-way ANOVA: df = 2, F = 7.772, p = 0.003). No branch-specific rate shifts are consistently associated with the K-Pg or PETM events, but the Cretaceous timing of crown Marsupialia and Placentalia shifts is consistent with the Early Rise model (Figure 4A, shifts A, C).

Tempo of the genus-level fossil record

Following a 100–80 Ma burst of origination and extinction involving lineages of extinct clades (e.g., multituberculates, cimolestans), the ~66-Ma K-Pg and ~56-Ma PETM events appear to have influenced the fossil record of crown Mammalia (Figure 2B). We find that at least 203 fossil genera originated during the Cretaceous prior to the K-Pg boundary, most of which are assigned to stem lineages of Monotremata, Theria, Marsupialia, and Placentalia. However, 3 Cretaceous lineages are highlighted for being possible members of crown Placentalia (Figure 2B): (1) *Deccanolestes* (Adapisoriculidae; range: 69.9–66 Ma) as either stem Afrotheria or stem Euarchontoglires,[43–45] (2) *Altacreodus* (possible "Creodonta"; 69.9–66 Ma) as stem Laurasiatheria,[46] and (3) some members assigned to "Condylarthra" such as *Paleoungulatum* (69.9–66 Ma), *Protungulatum* (69.9–65.1 Ma), and *Baioconodon* (69.9–63.1 Ma) as stem or crown Laurasiatheria.[45,47–49] Nevertheless, considerable debate underpins the phylogenetic placement of these fossils (e.g., Manz et al.[50]).

Cenozoic fossil diversification rates roughly follow the genus richness curves, with the highest increase of l occurring in the

A Extant timetree: reconstructed lineages


B Fossil record: genus durations
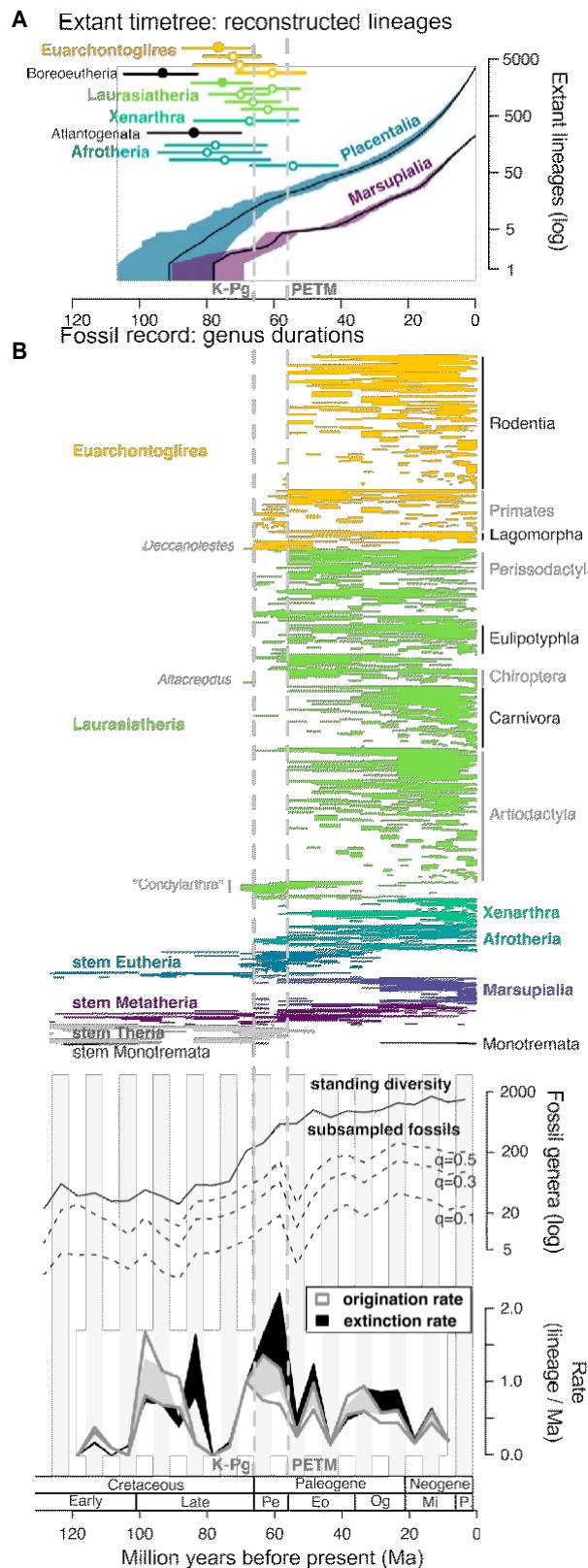
Figure 2. Diversification of mammal lineages relative to the Creta-ceous-Paleogene (K-Pg) boundary and Paleocene-Eocene Thermal Maximum (PETM)

Temporal dynamics are compared as reconstructed in the fossil-calibrated extant timetree (A) versus observed in the genus-level fossil record (B).

(A) Lineage-through-time plot of placentals and marsupials over 100 trees (thin black line is consensus tree) relative to the timing of the first 16 superordinal divergences of placentals (mean crown ages and 95% highest posterior density, HPD; filled circle if 95% HPD does not overlap the K-Pg boundary).
(B, top) Paleontological durations from first to last occurrence for all genera in crown Mammalia as recorded in the Paleobiology Database (n = 5,320 unique genera from 72,579 observations). Putative crown placental taxa recovered prior to the K-Pg boundary are highlighted in light gray (see Tempo of the genus-level fossil record). (B, middle) The richness of fossil generic diversity is shown through time as binned in 5 million year, Ma, intervals from 131–1 Ma (taxa spanning boundaries go in both bins) and subsampled using shareholder quorum sizes (q) of 0.5, 0.3, and 0.1 to maximize the uniformity of coverage. (B, bottom) Rates of fossil genus origination and extinction estimated using six different rate metrics and presented as confidence intervals from the low to high estimate in each 5-Ma bin (shaded polygons). Binned richness and rate data are plotted at the midpoint of each 5-Ma bin. Note that fossil coverage was insufficient for estimating rates in the most recent bin (6–1 Ma), and only the "second-for-third" metric could calculate rates for the 71–66 Ma bin. PETM, dashed gray lines; Paleocene, Pe; Eocene, Eo; Oligocene, Og; Miocene, Mi; Pliocene, P. See also Figure S2 and Tables S1, S3, S4, and S5.

66–61 Ma time bin (range of 6 rate metrics: 0.74–1.36 lineages/ Ma) and m in the 61–56 Ma bin (range: 0.89–2.20 lineages/Ma), with both rates stabilizing to ~0.5 (range: 0.16–0.88) lineages/ Ma from 20 Ma to the present (Figure 2B; Figure S2; Table S4). The Paleocene (66–56 Ma) surge of l and m apparent in the fossil record involves the origination of 495 genera between the K-Pg and PETM events, of which ~82% went extinct before the start of the Eocene ~56 Ma (408 genera). Of those extinctions, over 38% were within 1 Ma of the ~56 Ma PETM event when per genus durations are examined directly (157 genera). Only 26.9% of the Paleocene-originating taxa (113 genera) are allocated to the stem or crown of extant taxonomic orders (Eulipoty-phla, Macroscelidea, Primates, Perissodactyla, and Rodentia each with 10 or more representatives), indicating that nearly three-quarters of the total K-Pg-to-PETM originations did not leave closely related modern descendants. Alternatively, if we conservatively assign all Paleocene "Condylarthra" to stem Artiodactyla or Perissodactyla (e.g., phenacodontids[51]), then the fraction that are not allocated to extant taxonomic orders de-ceases to about two-thirds.

Subsampled genus richness reaches an early peak in the 61–56 Ma bin, just prior to the PETM, and then falls by ~80% in the next bin before recovering with a 3-fold increase in the 51–46 Ma bin (Figure 2B; Table S3). Raw richness importantly misses this major drop in taxonomic diversity, indicating non-uniform sam-pling of these fossil strata. Overall peak subsampled richness is consistently found in the 26–21 Ma time bin (late Oligocene–early Miocene; Figure 2B) as associated with the highest evenness of any interval (Shannon's H = 6.515; Table S3). Subsampled richness then declines by ~15% in the next bin and remains roughly flat until the most recent bin (Figure 2B; Table S3). Raw genus richness remarkably parallels the stability of subsampled richness since the Oligocene-Miocene transition ~23 Ma, underscoring the uniformity Miocene-Recent fossil sampling. Fully 27% of now-extant genera of mammals have fossil records older than 1 Ma (n = 351 of 1,283 genera in the

A Extant timetree: early crown orders

B Order-wide timetree diversification
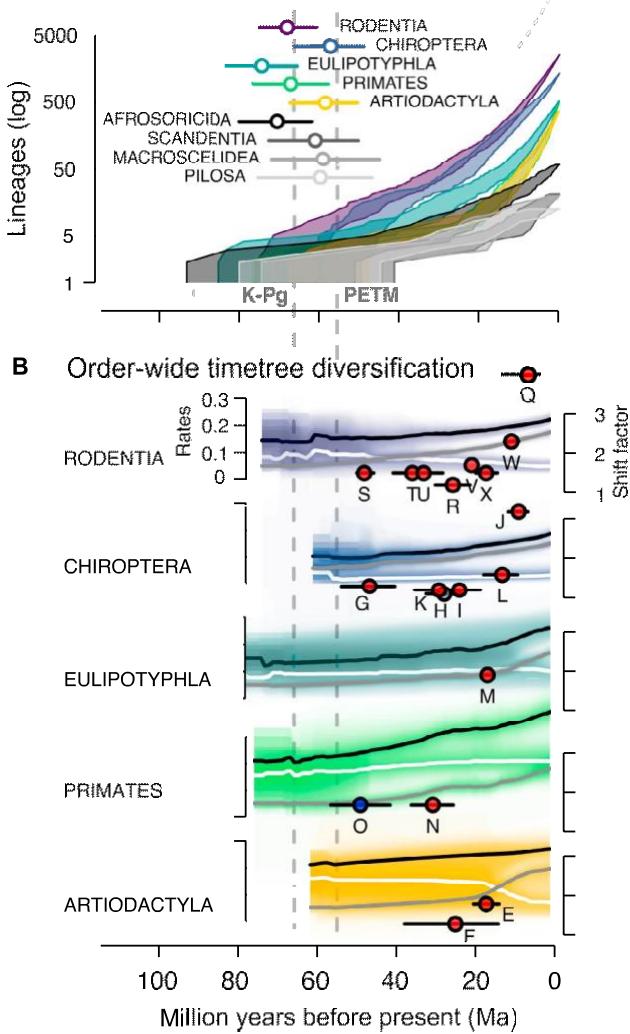
Figure 3. Diversification of early crown orders of mammals using the extant timetree

(A) Lineage-through-time plots and divergence times for all placental orders with crown radiations starting near the Cretaceous-Paleogene boundary (K-Pg) and Paleocene-Eocene Thermal Maximum (PETM; dashed gray lines). Divergence time means are shown with 95% highest posterior density (HPD) intervals. Colors correspond to the taxonomic orders shown in (B).

(B) Rates of speciation (black), extinction (white), and net diversification (gray) through time in the five most speciose early crown orders, as calculated in BAMM, as well as corresponding branch-specific shifts in net diversification (median rates from 10 trees, 95% error intervals in colors). The last 2 Ma are removed to focus on pre-recent rate dynamics. See also Figure S1 and Tables S1, S2, and S5.

timetree taxonomy), demonstrating continuity between fossil-and timetree-based investigations.

Pushing the pulled speciation rates

The calculation of pulled speciation rates, l_p, using extant time-trees recovers per-interval 95% CIs that include zero from 111–76 Ma, indicating that we are only confident of non-zero l_p beginning at ~71 Ma when a rate of 0.083 lineages/Ma (95% CI: 0.027–0.198) is recovered (Figure 4B; Table S5). After an

A Extant timetree rates through time

B Fossil correction of speciation rates
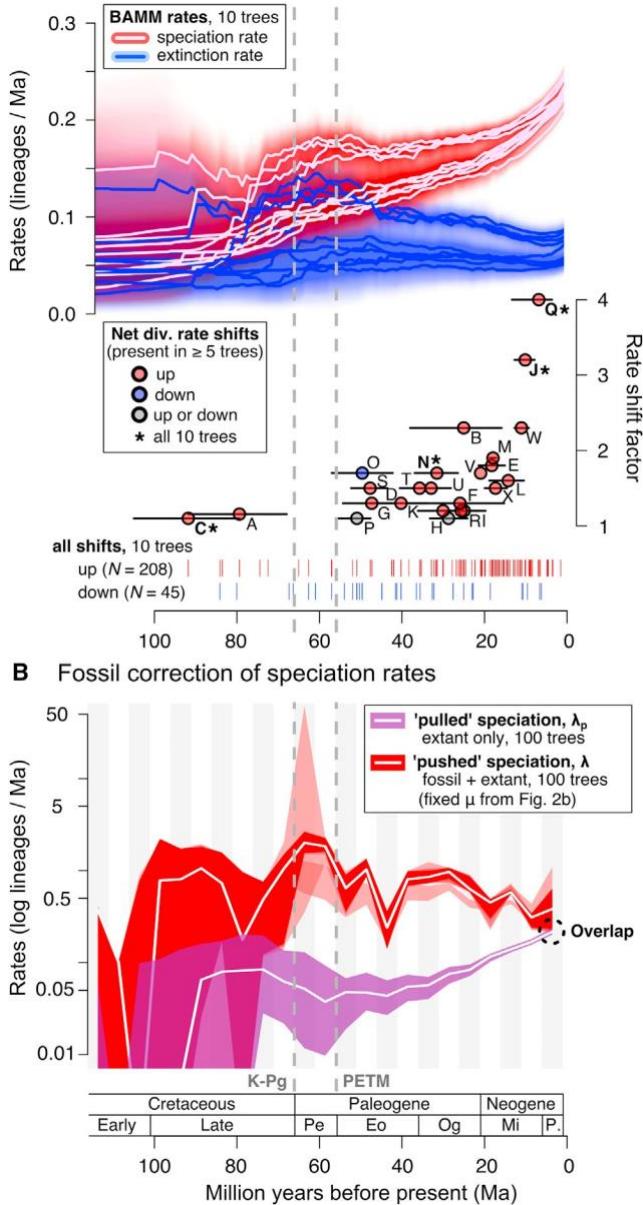
Figure 4. Rates of mammal diversification estimated considering the fossil record or not, as shown relative to the Cretaceous-Paleogene (K-Pg) boundary and Paleocene-Eocene Thermal Maximum (PETM)

(A, top) Inferred variation in rates of speciation, extinction, and net diversification upon 10 mammal timetrees using BAMM (shown are median rates and 95% confidence intervals (CIs) from each tree drawn from the credible set; the last 2 million years, Ma, are removed to focus on pre-recent rate dynamics). (A, bottom) Of the 253 possible shifts in branch-specific net diversification rates recovered, 24 were present in at least five of the ten trees (A–X; symbols match Figure 1) and 4 shifts were present in all trees (asterisks). (B) Pulled speciation rates, l_p, estimated over 100 timetrees at 5-Ma bins (purple; 95% CI and median in white) and then corrected or "pushed" as an estimate of true speciation rates, l (shades of red; 95% CI for each of 6 methods used to push the rates, with the grouped median shown in white). Note the log scale of l_p and l. The homogeneous birth-death modeling of l across each tree was performed by fixing the extinction rates, m, according to the 6 metrics of fossil extinction rate displayed in Figure 2B and repeating each estimate of l across 100 timetrees. The K-Pg and PETM are shown with dashed gray lines. See also Figures S1–S3 and Tables S2, S4, and S5.

A Tip rates comparison: 20 extant clades

$0.02 + 0.78x \; ; R^2 = 0.39$
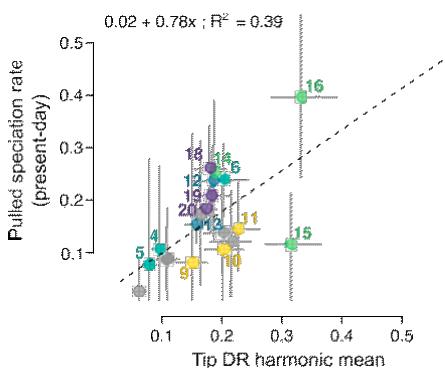
B Rate shifts versus tip-rate skewness

$-0.15 + 3.28x \; ; R^2 = 0.48$
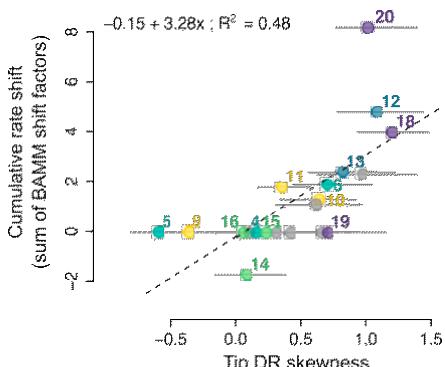
C Within-clade tip rate variation
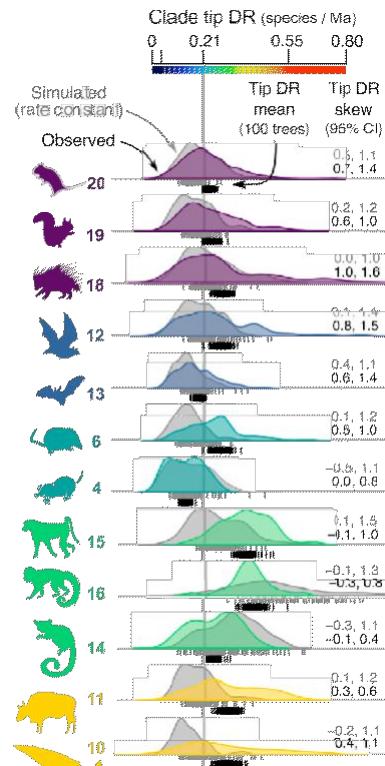
Figure 5. Present-day (tip) rates of speciation across and within mammal clades Comparison of 20 mammal clades following the delimitation in Figure 1, showing clades numbered from the five most speciose orders.

(A) Pulled speciation rates at the instantaneous present (l_0) for each clade as compared to the harmonic mean of species' tip DR values in those clades (95% confidence intervals, CIs, in gray; linear model is given).

(B) The cumulative total of BAMM rate shift factors within each clade as compared to that clade's skewness of species' tip DR values (95% CIs for the clade tip DR skew across 10,000 mammal trees; linear model is given).

(C) Rate variation within clades of the five most speciose orders, showing species' tip DR distributions for the empirically reconstructed phylogenies of mammals (colors) versus simulated trees of the same species richness using a rate-constant birth-death model (gray). Density plots of tip DR from one empirical and one simulated tree are shown as examples relative to the 100-tree calculations of clade tip DR mean (black and gray ticks) and skew (95% CIs). See also Table S6.

apparent subsequent decline in the median from 66–56 Ma, pulled speciation rates rise steadily to a modern peak of 0.216 lineages/Ma (0.201–0.237) at 6–1 Ma. By comparison, the tree-wide estimate of l_0 at the present day is 0.217 lineages/Ma (0.197–0.239), and the tree-wide median of species' tip DR is 0.206 species/Ma (95% CI: 0.055–0.476), with higher variability due to the per-species estimation of values.

Because older values of l_p are pulled downward by un-sampled lineages, they are biased relative to their true values, l.[20] Efforts to push the estimated speciation rates back to l yield differing results depending on whether we fix fossil extinction rates or the total extant lineages through time (Figure S3). We favor using fixed extinction rates as they allow estimated uncertainty across 6 different metrics to be integrated into the pushed speciation rate analyses. Using the fixed extinction rates, we importantly find that the K-Pg-to-PETM interval includes both the lowest value of pulled rates (0.037 lineages/ Ma; 95% CI: 0.009–0.092) and the highest value of pushed rates (median of 2.0 lineages/Ma; 0.608–24.487; Figure 4B). Moreover, the molecular timetree (pulled) and fossil-corrected (pushed) rates of speciation begin converging ~10 Ma (11–6 Ma bin) with estimates that overlap in the 6–1 Ma bin, indicating that they are statistically indistinguishable near the present (Figure 4B). Overall, the pushed rates of speciation are on average 14-fold higher than the pulled rates, ranging from a peak 50-fold difference in medians near the PETM to a 1.7-fold difference toward the present (Table S5), which is consistent with expectations that fewer unsampled extinctions result in less bias nearer to timetree tips.

the instantaneous present, l_0, show a strong positive relationship with the clade harmonic mean of species' tip DR values ($R^2 = 0.39$, p = 0.003; Figure 5A). Hence, tip DR calculated under the modern sampling fraction of 1.0 approximates $r l_0$, a quantity that was shown to be identifiable.[20,21] Comparing clade-level skewness of tip DR to the cumulative rate shift of each clade (sum of BAMM rate-shift factors for independent shifts; Tables S2 and S6) also reveals a strong positive relationship ($R^2 = 0.48$, p < 0.001; Figure 5B). Tip DR skewness thus offers a simple, approximate means of assessing the likelihood that a shift in net diversification rates occurred in that clade's recent history.

The intuition of tip DR skewness is clear upon plotting observed distributions of clade tip DR relative to expected values under rate-constant birth-death processes (Figure 5C; Table S6). The clades with the largest magnitude rate-shifts such as guinea pig-related rodents (clade 18, shift Q) and Yinpterochiroptera (clade 12, shift J) also show the highest tip DR skewness (Figures 5B and 5C). Beyond statistical moments, the tip DR distribution offers an intriguing summary of the clade-wide, among-species variation in speciation rates, ranging from broad in Old and New World monkeys (clades 15, 16) to multi-peaked in true moles and lemur-related primates (clades 4, 14, Figure 1).

Comparing pulled rates, tip-level rates, and rate shifts

Considering rate summaries across the 20 extant clades delimited in Figure 1, we find that pulled speciation rates at

DISCUSSION

We find diversification-rate signatures in the mammal fossil record and extant timetrees that are distinct yet complementary in the stories they tell. Fossil rates provide greater insights for

deep-time questions while molecular timetree rates are increasingly consistent with the fossil information toward the present. Timetrees offer richer, species-level coverage and associated insights of modern ecological diversity that are lacking in the fossil record. When combined for mammals, the two speciation-rate sources begin to converge starting ~10 Ma but overlap in the most recent time bin (Figure 4B), consistent with species' tip rates being unbiased estimators of recent speciation processes (Figures 1 and 5A). These results are in accord with theoretical work[20,22] regarding the accumulation of unrecorded extinctions in extant timetrees, which causes increasing bias for deeper-time rate dynamics as lineages are progressively erased.

The K-Pg mass extinction ~66 Ma is found to precede a surge of fossil genus turnover (origination + extinction; Figure 2B) and frame a bevy of timetree divergences that overlap in age with either the K-Pg event or ensuing PETM ~56 Ma (Figures 1 and 2A). However, none of those timetree divergences are recovered as branch-specific shifts in net diversification rate (Figures 3B and 4A), counter to expectations for novel macroevolutionary regimes (sensu Rabosky[28]) to be timetree detectable in response to major geobiotic events. Combining fossil and extant rate information, our analyses support both the Suppression and Delayed Rise models of diversification[31,33,35]: diversity recoveries following the K-Pg and PETM events were milestones in the radiation of mammals (Figure 4B). Elevated fossil diversification ~100–80 Ma (Figure 2B) is also consistent with the early side of the Early Rise model but more in the context of lineage turnover and regional effects of now-extinct or -depauperate clades[52] rather than the rise of extant mammal radiations. Fossil-corrected rates from this Cretaceous period are highly uncertain (Figure 4B), presumably because only a few early rising lineages survived to be represented in the timetree. Comparing fossil- and timetree-based perspectives thus establishes that these models of deep-time diversification are not mutually exclusive; yet, if only extant timetree lineages are considered, the concentration of Eocene and Oligocene rate shifts tells a Delayed Rise-focused story.

As predicted,[20,22] rates of speciation estimated across the molecular timetree are pulled downward in magnitude for the same intervals in which extinction events have erased lineages from the timetree. The largest extinction-rate increase is recorded in fossil mammals prior to the PETM ~56 Ma (Figure 2B), an event apparently triggered by the anomalous spike in global temperatures.[37] Concurrent with those extinctions is a substantial dip in the tree-wide pulled speciation rates, which results in rate estimates of 50-fold greater magnitude when those pulled rates are pushed by fossil lineage-level extinction rates (Figure 4B). Hence, on their own, the backbone-and-patch timetrees of mammals do not record the Paleocene pulse (K-Pg to PETM) in turnover that fossil durations show, a finding that helps to explain the absence of any explosive K-Pg signature in most mammal phylogenetic studies,[13,31,40,53–55] but see O'Leary et al.[47] and Phillips and Fruciano.[56]

Neontologists have long searched for the "smoking gun" of K-Pg-driven radiations in molecular timetrees, but perhaps they have been looking in the wrong place. Finding such a rate signature is only expected if lineages that originated near the K-Pg event survived until the present. For mammals, the fossil record shows the selective extinction of ecological specialists

at the end-Cretaceous, both in North America[41,57–60] and globally,[34] followed by a Paleocene rebound in taxonomic richness dominated by the now-extinct stem lineages of crown orders (e.g., archaic ungulates, leptictids, plesiadapiforms, creodonts, and mesonychids[34,35,41,45,60]). The stemward placement of most Paleocene placental fossils[45] supports the hypothesis that K-Pg-associated diversification signatures were lost from the branching pattern of mammal molecular timetrees, as does the pre-PETM extinction of nearly two-thirds of taxa that originated in the Paleocene pulse (Figure 2B). Thus, many aspects of mammalian diversification history are not knowable from extant timetrees alone. Extant timetree-based inference of the rate dynamics near ancient events like the K-Pg and PETM may rightly be viewed as impossible to ascertain,[15,26] making the fossil record indispensable for understanding deep-time evolutionary questions.

Tip rates and their clade-wide moments as an identifiable path forward

Thankfully, modern timetrees are not devoid of rate information, despite some important biases[15,20] and some headlines to the contrary.[61] We show that molecular timetree- and fossil-corrected rate estimates (pulled versus pushed) are congruent near the present day (Figure 4B), a finding that reinforces the use of tip rates as an identifiable means of investigating recent evolutionary processes, at least when extant taxon sampling is known. Louca and Pennell[20] established a formal proof and clear explication of how unobserved lineages (both extinct and extant) can render timetree rate inferences non-identifiable, extending previous theoretical and empirical work.[15,22,26,62,63] By using completely sampled extant phylogenies, tip rates of speciation can be estimated using non-parametric approaches (e.g., the tip DR method we use here, or the coarser metric of node density[29,64]) that are computationally scalable across samples of timetrees and thus able to account for phylogenetic uncertainty. In contrast, parametric methods of calculating tip rates do not scale well across tree samples but can be more accurate under some diversification scenarios (see Title and Rabosky[30]).

Tip-rate insights are importantly not limited to present-day environments: we show that the skewness of tip DR distributions across 20 mammal clades is predictive of their historical extent of branch-specific rate shifts identified using BAMM (Figures 5B and 5C). That is, the clade-level distributions of species' tip speciation rates approximate rate dynamics estimated using a formal birth-death process model. This suggests that tip-rate skewness alone can identify timetree rate shifts, analogous to how non-parametric tests of trait-dependent speciation are conducted (e.g., FiSSE, ES-sim[65,66]). Establishing a null distribution of the test statistic (e.g., the clade-level skewness of tip rates given trees simulated under birth-death) will allow comparisons between observed and expected tip-rate skewness. Our initial trials of this test find that empirical tip DR distributions tend to be more right skewed and with higher mean values than expected by chance (Figure 5C; Table S6). A fuller exploration of simulation parameters is needed to formalize this approach, but these initial results are promising. The most common approaches to measuring clade-level diversification, including BAMM and others, provide summarized rate information only for clades or rate regimes. Capturing skewness and other

moments from clade-wise tip DR distributions offers more nuanced avenues for quantitative as well as visual inference that might unmask patterns not readily conveyed using parametric approaches.

Reconciling timetree rate shifts: When are they believable?

The above discussion raises the question: when do branch-specific rate shifts in timetrees reflect historical changes in macro-evolutionary regime versus artifacts of unsampled extinction? Our finding that rate shifts are concentrated in the mammal time-trees since ~50 Ma, including eight shifts detected from 50–30 Ma (Figures 1 and 4A), is consistent with the post-PETM, mid-to-late Eocene radiations of crown Carnivora and suborders of primates, rodents, bats, and marsupials. Collectively, these crown radiations expanded the taxonomic and eco-morphological diversity of modern mammals.[35] However, as mentioned above, their stem lineages are known to have originated and gone extinct earlier in the Cenozoic (e.g., creodonts potentially allied with Carnivora, plesiadapiforms allied with Primates). If those stem lineages were sampled in the timetree, presumably each "shift" to higher net diversification rates would appear less abrupt, perhaps showing no detectable change in macro-evolutionary regime, or perhaps showing that less frequent extinction rather than faster speciation underpin some rate shifts (e.g., Lloyd and Slater[25]). Conversely, groups like horses[67] that declined in diversity since the Miocene show diversification-rate stasis from an extant timetree perspective.[68,69] Thus, without aid from the fossil record, we find an artifactual view of deep-time diversification dynamics.

By contrast, we expect branch-specific rate shifts to carry a greater signal of real biological processes toward the present. In mammals we see such convergence begin ~10 Ma, which is not only when pulled speciation rates start converging with fossil-corrected estimates (Figure 4B) but also when rate shifts show the greatest magnitude and consistency in signal across sampled timetrees (Figure 4A). Strikingly, the two largest rate increases (4.03 and 3.23) occurred in the last ~10 Ma in clades with very disparate life modes: the fossorial tuco-tucos of South America (*Ctenomys*, Q), and the flying foxes of Indo-Pacific islands (*Pteropus*, J; Figures 1, 3B, and 4A). Small burrowers and large flyers both show similar signatures of recent and rapid net diversification under conditions of insularity, although in sub-terranean and oceanic realms, respectively, suggesting that their similar propensities for geographic isolation may be driving these dynamics. The role of allopatry in mammal speciation has long been noted as the predominant pattern among closely related species (e.g., Baker and Bradley[70]), and vagility differences appear to be inversely related to speciation rates in some taxa (e.g., Claramunt et al.[71]). However, how traits of low and high vagility (burrowing and flying, respectively) might interact with different scales of insular habitat matrix to produce similar out-comes is less well explored (but see Kisel and Barraclough[72]). We hypothesize that apparently large rate shifts like Q and J may in reality be more common than is detectable in extant timetrees, especially if speciation and extinction rates are temporally coupled.[73] Yet with the fragmentary information at hand, including many unsampled extinctions even when fossils are added, all efforts to detect macroevolutionary rate disjunctions

will first need to reckon with the likelihood that enough diver-gence events have been sampled to recover robust rate signals.

We see two main paths of recourse regarding when to trust rate-shift analyses in extant timetrees: (1) evaluate results rela-tive to parallel evidence (e.g., fossils, demography, eco-geographic context), especially for older rate shifts: if multiple lines of evidence support a shift, it is more likely to be real, and (2) focus on understanding which common causes may underlie shift dynamics in younger clades for which presumably fewer un-sampled extinctions are affecting rate estimates. When working with younger clades, the possibility that young clades might actually have inherently faster rates than older clades should also be tested. Although this time-dependent rates hypothesis currently lacks a mechanism, it appears robust to fossil and mo-lecular data types,[74] which show gradual, tree-wide increases in both speciation and extinction rates. Alternatively, detecting larger rate shifts nearer to the present, as we did in mammals, may suggest a different picture whereby uncharacterized eco-evolutionary accelerators (e.g., species traits, environmental fac-tors) are causing exceptional clade-specific radiations, either in addition to or instead of time dependence. In the latter case, apparent time dependence may be an artifact of rare but excep-tional clade-specific radiations relative to a broader taxon. Such exceptional radiations need not have adaptive drivers, though that is a possibility.[75]

Reconciling previous mammal studies: What do we actually know?

In light of our joint insights from the backbone-and-patch time-trees and fossil record, there is a critical need to re-evaluate what aspects of previous studies of extant mammal diversification can be deemed reliable. Two influential mammal phylogenies have been used to address similar questions of branch-specific rate shifts[32,76]: the largely species-level supertree of Bininda-Emonds et al.[31] and the family-level supermatrix timetree of Meredith et al.[13] These trees differ from backbone-and-patch timetrees investigated here by collapsing topological and age uncertainty into a consensus phylogeny and, in the case of the supertree approach, losing branch lengths whenever information from merged subclades disagreed.[2]

The 24 branch-specific shifts in net diversification we recover in the backbone-and-patch timetrees (Figures 1, 3B, and 4A) compared to 27 shifts detected in the supertree (15 up-shifts, 12 down-shifts[32]) and 9 up-shifts in the supermatrix timetree.[76] To their credit, Purvis et al.[32] analyzed only 1,335 bifurcating nodes in the supertree, which avoided some rate artifacts of polyt-omies. However, both studies returned overconfident estimates by treating the consensus phylogeny as known without error.[77] If we only compare up-shifts, given the likely erasure of extant lineages as net diversification slows down,[17,78,79] we find three lineages shared by our study, Purvis et al.,[32] and Yu et al.[76]: (1) Placentalia (or one branch forward at Boreoeutheria), (2) Simiiformes (Primates, New and Old World monkeys), and (3) Macropodidae (Diprotodontia, kangaroos, and wallabies). The commonality of those shifts argues that their evolutionary-rate signatures are robust to different models of phylogenetic reconstruction (supertree versus supermatrix versus Bayesian backbone-and-patch) and rate inference (SymmeTree versus MEDUSA versus BAMM). Of these, the Macropodidae shift is

the youngest, recovered in our study at ~15 Ma (12.2–18.0), and thus the least likely to be biased by unsampled extinctions. Previous fossil and molecular analyses suggest that kangaroo genus-level divergences may be driving this shift.[80,81]

At shallower phylogenetic levels, other studies have found rate shifts similar to those we infer. For example, the Cetacea shift (F in Figure 1) was previously recovered two branches forward on the branch leading to oceanic dolphins.[25,28,82] Similarly, the Simiiformes shift (N) was recovered two branches forward (Cercopithecidae[83]) and the Ctenomyidae shift (Q) two branches back (Octodontoidea excluding Abrocomidae[84]). In contrast, the six rate shifts we found in bats (G–L, Figure 1) compared to two shifts previously recovered (shifts H, J[85]). We suggest that high topological uncertainty in bats[86] contributes to equivocal modeling of branch-specific processes. Therein lies a paradox: pinpointing rate-shift signatures is difficult in clades that are difficult to resolve, and resolving clades may be hardest in cases of recent, rapid radiation, in which signals of incomplete lineage sorting and hybridization are expected to be strongest.[87] Thus, rather than relying on phylogenomic data to yield greater resolution, comparative methods also need to develop more meaningful ways of handling phylogenetic uncertainty.

Caveats to the pushing of pulled speciation rates

Approaches to using the fossil record to correct or push the pulled rates of speciation estimated from extant timetrees are nascent but offer a promising means of parsing plausible diversification scenarios.[20] We here applied two approaches to this problem: fixing E(t), the total number of extinct and extant lineages through time, and fixing m(t), the fossil-estimated extinction rate through time using different rate metrics. While the latter approach returned more realistic speciation-rate estimates (Figure S3), we highlight that both approaches could be substantially improved. For example, among-bin heterogeneity in fossil sampling probabilities could be incorporated into rate models,[12,88] which should make the estimation of E(t) and m(t) more robust. Similarly, using a fossil phylogenetic approach would add expected ghost lineages among genera, even if coarse taxonomic assignments are used as a proxy for cladistic data (e.g., Lloyd and Slater,[25] Smits,[89] and Soul and Friedman[90]).

There are known issues with the fidelity of stratigraphic and taxonomic assignments in compiled fossil data, including in the Paleobiology Database (e.g., Prothero[91]), which have added noise to our analyses. Our efforts to improve public data by integrating curated snapshots by geological time interval[41,45,92] and fossil taxon[46,93,94] are critical but importantly also highlight the need to incentivize ongoing public curation of paleontological resources. Despite these concerns, our view is that paleontological biases are far less systematic than those that emerge from conducting deep-time rate inferences without considering unsampled extinctions. Hence, any addition of fossil data to extant phylogenetic analyses is likely to provide greater macroevolutionary realism.

Conclusions

Overall, our results indicate that extant timetrees contain sufficient evolutionary-rate information for approximately unbiased investigation at levels of species tips to shallow clades (e.g., ~10-Ma stem age or younger). Extant taxon sampling must be complete or at least completely modeled while accounting for non-random (e.g., geographically biased) sampling. When interpreting results, the probability of bias from clade-, region-, or ecotype-specific extinctions must also be considered. We emphasize that fossil and living organisms record signatures of the same evolutionary processes, just from very different temporal viewpoints. Debating "rocks versus clocks" as the ultimate arbiters of evolutionary history misses the point of their interdependence. Timetrees and fossils are like the bow and stern of an evolutionary ship sailing through the sea of time; as the bow cuts through the recent past and probable future of biodiversity processes, it leaves behind fossils in its wake. Traces of the past may or may not help navigate the future, but they nevertheless illuminate our evolutionary trajectory. Harnessing these complementary data sources should allow us to realize the strengths of timetrees (recent processes) alongside those of fossils (ancient processes) toward establishing a fuller understanding of evolutionary history. Future work to query the causal impact of deep-time events like the K-Pg or PETM upon diversification rates should merge fossil and living diversity into phylogenetic analyses, or else be viewed with caution. In turn, fossil-free timetrees should be prioritized for application to shallow-time questions for which species-level lineages can be fully sampled and meaningfully analyzed relative to hypothesized covariates.

STAR+METHODS

Detailed methods are provided in the online version of this paper and include the following:

- d KEY RESOURCES TABLE
- d RESOURCE AVAILABILITY
  - B Lead contact
  - B Materials availability
  - B Data and code availability
- d METHOD DETAILS
  - B Mammalian phylogeny
  - B Fossil genus durations
- d QUANTIFICATION AND STATISTICAL ANALYSES
  - B Branch-specific rate shifts
  - B Comparisons with fossil genus diversification
  - B Speciation rates
  - B Fossil-correction of pulled speciation rates

AUTHOR CONTRIBUTIONS

N.S.U. and W.J. conceived the study; N.S.U. and J.A.E. collected and curated the data; N.S.U. performed all analyses and wrote the first draft of the manuscript, with revisions from all co-authors.

DECLARATION OF INTERESTS

The authors declare no competing interests.

REFERENCES

1. Burgin, C.J., Colella, J.P., Kahn, P.L., and Upham, N.S. (2018). How many species of mammals are there? J. Mammal. *99*, 1–14.

2. Upham, N.S., Esselstyn, J.A., and Jetz, W. (2019). Inferring the mammal tree: Species-level sets of phylogenies for questions in ecology, evolution, and conservation. PLoS Biol. *17*, e3000494.

3. Davies, T.W., Bell, M.A., Goswami, A., and Halliday, T.J.D. (2017). Completeness of the eutherian mammal fossil record and implications for reconstructing mammal evolution through the Cretaceous/Paleogene mass extinction. Paleobiology *43*, 521–536.

4. Bennett, C.V., Upchurch, P., Goin, F.J., and Goswami, A. (2018). Deep time diversity of metatherian mammals: implications for evolutionary history and fossil-record quality. Paleobiology *44*, 171–198.

5. Osborn, H.F. (1902). The Law of Adaptive Radiation. Am. Nat. *36*, 353–363.

6. Simpson, G.G. (1944). Tempo and Mode in Evolution (Columbia Univ. Press).

7. Vrba, E.S. (1992). Mammals as a Key to Evolutionary Theory. J. Mammal. *73*, 1–28.

8. Alroy, J., Uhen, M.D., Mannion, P.D., Jaramillo, C., Carrano, M.T., and van den Hoek Ostende, L.W. (2018). Taxonomic occurrences of Mammalia recorded in Fossilworks, the Evolution of Terrestrial Ecosystems database, and the Paleobiology Database. Fossilworks. http://fossilworks.org.

9. Scornavacca, C., Belkhir, K., Lopez, J., Dernat, R., Delsuc, F., Douzery, E.J.P., and Ranwez, V. (2019). OrthoMaM v10: Scaling-Up Orthologous Coding Sequence and Exon Alignments with More than One Hundred Mammalian Genomes. Mol. Biol. Evol. *36*, 861–862.

10. Hunt, G., and Slater, G. (2016). Integrating Paleontological and Phylogenetic Approaches to Macroevolution. Annu. Rev. Ecol. Evol. Syst. *47*, 189–213.

11. Hopkins, M.J., Bapst, D.W., Simpson, C., and Warnock, R.C.M. (2018). The inseparability of sampling and time and its influence on attempts to unify the molecular and fossil records. Paleobiology *44*, 561–574.

12. Silvestro, D., Warnock, R.C.M., Gavryushkina, A., and Stadler, T. (2018). Closing the gap between palaeontological and neontological speciation and extinction rate estimates. Nat. Commun. *9*, 5237.

13.

14. Oliveros, C.H., Field, D.J., Ksepka, D.T., Barker, F.K., Aleixo, A., Andersen, M.J., Alström, P., Benz, B.W., Braun, E.L., Braun, M.J., et al. (2019). Earth history and the passerine superradiation. Proc. Natl. Acad. Sci. USA *116*, 7916–7925.

15. Marshall, C.R. (2017). Five palaeobiological laws needed to understand the evolution of the living biota. Nat. Ecol. Evol. *1*, 165.

16. Maddison, W.P., Midford, P.E., Otto, S.P., and Oakley, T. (2007). Estimating a binary character's effect on speciation and extinction. Syst. Biol. *56*, 701–710.

17. Moore, B.R., Höhna, S., May, M.R., Rannala, B., and Huelsenbeck, J.P. (2016). Critically evaluating the theory and performance of Bayesian analysis of macroevolutionary mixtures. Proc. Natl. Acad. Sci. USA *113*, 9569–9574.

18. Rabosky, D.L., Mitchell, J.S., and Chang, J. (2017). Is BAMM flawed? Theoretical and practical concerns in the analysis of multi-rate diversification models. Syst. Biol. *66*, 477–498.

19. Benson, R.B.J., and Mannion, P.D. (2012). Multi-variate models are essential for understanding vertebrate diversification in deep time. Biol. Lett. *8*, 127–130.

20. Louca, S., and Pennell, M.W. (2020). Extant timetrees are consistent with a myriad of diversification histories. Nature *580*, 502–505.

21. Louca, S., Shih, P.M., Pennell, M.W., Fischer, W.W., Parfrey, L.W., and Doebeli, M. (2018). Bacterial diversification through geological time. Nat. Ecol. Evol. *2*, 1458–1467.

22. Lambert, A., and Stadler, T. (2013). Birth-death models and coalescent point processes: the shape and probability of reconstructed phylogenies. Theor. Popul. Biol. *90*, 113–128.

23. Heath, T.A., Huelsenbeck, J.P., and Stadler, T. (2014). The fossilized birth-death process for coherent calibration of divergence-time estimates. Proc. Natl. Acad. Sci. USA *111*, E2957–E2966.

24. Stadler, T., Gavryushkina, A., Warnock, R.C.M., Drummond, A.J., and Heath, T.A. (2018). The fossilized birth-death model for the analysis of stratigraphic range data under different speciation modes. J. Theor. Biol. *447*, 41–55.

25. Lloyd, G.T., and Slater, G.J. (2021). A Total-Group Phylogenetic Metatree for Cetacea and the Importance of Fossil Data in Diversification Analyses. Syst. Biol. syab002.

26. Quental, T.B., and Marshall, C.R. (2010). Diversity dynamics: molecular phylogenies need the fossil record. Trends Ecol. Evol. *25*, 434–441.

27. Morlon, H., Parsons, T.L., and Plotkin, J.B. (2011). Reconciling molecular phylogenies with the fossil record. Proc. Natl. Acad. Sci. USA *108*, 16327–16332.

28. Rabosky, D.L. (2014). Automatic detection of key innovations, rate shifts, and diversity-dependence on phylogenetic trees. PLoS ONE *9*, e89543.

29. Jetz, W., Thomas, G.H., Joy, J.B., Hartmann, K., and Mooers, A.O. (2012). The global diversity of birds in space and time. Nature *491*, 444–448.

30. Title, P.O., and Rabosky, D.L. (2019). Tip rates, phylogenies and diversification: What are we estimating, and how good are the estimates? Methods Ecol. Evol. *10*, 821–834.

31. Bininda-Emonds, O.R.P., Cardillo, M., Jones, K.E., MacPhee, R.D.E., Beck, R.M.D., Grenyer, R., Price, S.A., Vos, R.A., Gittleman, J.L., and Purvis, A. (2007). The delayed rise of present-day mammals. Nature *446*, 507–512.

32. Purvis, A., Fritz, S.A., Rodríguez, J., Harvey, P.H., and Grenyer, R. (2011). The shape of mammalian phylogeny: patterns, processes and scales. Philos. Trans. R. Soc. Lond. B Biol. Sci. *366*, 2462–2477.

33. Osborn, H.F. (1910). The Age of Mammals in Europe, Asia and North America (Macmillan).

13. Meredith, R.W., Janečka, J.E., Gatesy, J., Ryder, O.A., Fisher, C.A., Teeling, E.C., Goodbla, A., Eizirik, E., Simão, T.L.L., Stadler, T., et al. (2011). Impacts of the Cretaceous Terrestrial Revolution and KPg extinction on mammal diversification. Science *334*, 521–524.

34. Grossnickle, D.M., and Newham, E. (2016). Therian mammals experience an ecomorphological radiation during the Late Cretaceous and selective extinction at the K–Pg boundary. Proc. Biol. Sci. *283*, 20160256.

35. Grossnickle, D.M., Smith, S.M., and Wilson, G.P. (2019). Untangling the Multiple Ecological Radiations of Early Mammals. Trends Ecol. Evol. *34*, 936–949.

36. Gingerich, P.D. (2006). Environment and evolution through the Paleocene-Eocene thermal maximum. Trends Ecol. Evol. *21*, 246–253.

37. Bowen, G.J., Maibauer, B.J., Kraus, M.J., Rö¨ hl, U., Westerhold, T., Steimke, A., Gingerich, P.D., Wing, S.L., and Clyde, W.C. (2015). Two massive, rapid releases of carbon during the onset of the Palaeocene–Eocene thermal maximum. Nat. Geosci. *8*, 44–47.

38. Wilson, G.P., Evans, A.R., Corfe, I.J., Smits, P.D., Fortelius, M., and Jernvall, J. (2012). Adaptive radiation of multituberculate mammals before the extinction of dinosaurs. Nature *483*, 457–460.

39. Archibald, J.D., and Deutschman, D.H. (2001). Quantitative Analysis of the Timing of the Origin and Diversification of Extant Placental Orders. J. Mamm. Evol. *8*, 107–124.

40. Springer, M.S., Foley, N.M., Brady, P.L., Gatesy, J., and Murphy, W.J. (2019). Evolutionary Models for the Diversification of Placental Mammals Across the KPg Boundary. Front. Genet. *10*, 1241.

41. Pires, M.M., Rankin, B.D., Silvestro, D., and Quental, T.B. (2018). Diversification dynamics of mammalian clades during the K-Pg mass extinction. Biol. Lett. *14*, 20180458.

42. Hull, P.M., Bornemann, A., Penman, D.E., Henehan, M.J., Norris, R.D., Wilson, P.A., Blum, P., Alegret, L., Batenburg, S.J., Bown, P.R., et al. (2020). On impact and volcanism across the Cretaceous-Paleogene boundary. Science *367*, 266–272.

43. Seiffert, E.R. (2010). The Oldest and Youngest Records of Afrosoricid Placentals from the Fayum Depression of Northern Egypt. Acta Palaeontol. Pol. *55*, 599–616.

44. Goswami, A., Prasad, G.V.R., Upchurch, P., Boyer, D.M., Seiffert, E.R., Verma, O., Gheerbrant, E., and Flynn, J.J. (2011). A radiation of arboreal basal eutherian mammals beginning in the Late Cretaceous of India. Proc. Natl. Acad. Sci. USA *108*, 16333–16338.

45. Halliday, T.J.D., Upchurch, P., and Goswami, A. (2017). Resolving the re-lationships of Paleocene placental mammals. Biol. Rev. Camb. Philos. Soc. *92*, 521–550.

46. Fox, R.C. (2015). A revision of the Late Cretaceous–Paleocene eutherian mammal Cimolestes Marsh, 1889. Can. J. Earth Sci. *52*, 1137–1149.

47. O'Leary, M.A., Bloch, J.I., Flynn, J.J., Gaudin, T.J., Giallombardo, A., Giannini, N.P., Goldberg, S.L., Kraatz, B.P., Luo, Z.-X., Meng, J., et al. (2013). The placental mammal ancestor and the post-K-Pg radiation of placentals. Science *339*, 662–667.

48. Kelly, T.S. (2014). Preliminary report on the mammals from Lane's Little Jaw Site quarry: A latest Cretaceous (earliest Puercan?) local fauna, Hell Creek Formation, southeastern Montana. Paludicola *10*, 42.

49. Archibald, J.D., Zhang, Y., Harper, T., and Cifelli, R.L. (2011). Protungulatum, Confirmed Cretaceous Occurrence of an Otherwise Paleocene Eutherian (Placental?). Mammal. J. Mamm. Evol. *18*, 153–161.

50. Manz, C.L., Chester, S.G.B., Bloch, J.I., Silcox, M.T., and Sargis, E.J. (2015). New partial skeletons of Palaeocene Nyctitheriidae and evalua-tion of proposed euarchontan affinities. Biol. Lett. *11*, 20140911.

51. Cooper, L.N., Seiffert, E.R., Clementz, M., Madar, S.I., Bajpai, S., Hussain, S.T., and Thewissen, J.G.M. (2014). Anthracobunids from the middle eocene of India and pakistan are stem perissodactyls. PLoS ONE *9*, e109232.

52. Benson, R.B.J., Mannion, P.D., Butler, R.J., Upchurch, P., Goswami, A., and Evans, S.E. (2013). Cretaceous tetrapod fossil record sampling and faunal turnover: Implications for biogeography and the rise of modern clades. Palaeogeogr. Palaeoclimatol. Palaeoecol. *372*, 88–107.

53. Stadler, T. (2011). Mammalian phylogeny reveals recent diversification rate shifts. Proc. Natl. Acad. Sci. USA *108*, 6187–6192.

54.

dos Reis, M., Inoue, J., Hasegawa, M., Asher, R.J., Donoghue, P.C.J., and Yang, Z. (2012). Phylogenomic datasets provide both precision and accuracy in estimating the timescale of placental mammal phylogeny. Proc. Biol. Sci. *279*, 3491–3500.

55. Liu, L., Zhang, J., Rheindt, F.E., Lei, F., Qu, Y., Wang, Y., Zhang, Y., Sullivan, C., Nie, W., Wang, J., et al. (2017). Genomic evidence reveals a radiation of placental mammals uninterrupted by the KPg boundary. Proc. Natl. Acad. Sci. USA *114*, E7282–E7290.

56. Phillips, M.J., and Fruciano, C. (2018). The soft explosive model of placental mammal evolution. BMC Evol. Biol. *18*, 104.

57. Wilson, G.P. (2013). Mammals across the K/Pg boundary in northeastern Montana, U.S.A.: dental morphology and body-size patterns reveal extinc-tion selectivity and immigrant-fueled ecospace filling. Paleobiology *39*, 429–469.

58. Longrich, N.R., Scriberas, J., and Wills, M.A. (2016). Severe extinction and rapid recovery of mammals across the Cretaceous-Palaeogene boundary, and the effects of rarity on patterns of extinction and recovery. J. Evol. Biol. *29*, 1495–1512.

59. Lyson, T.R., Miller, I.M., Bercovici, A.D., Weissenburger, K., Fuentes, A.J., Clyde, W.C., Hagadorn, J.W., Butrim, M.J., Johnson, K.R., Fleming, R.F., et al. (2019). Exceptional continental record of biotic re-covery after the Cretaceous-Paleogene mass extinction. Science *366*, 977–983.

60. Alroy, J. (1999). The fossil record of North American mammals: evidence for a Paleocene evolutionary radiation. Syst. Biol. *48*, 107–118.

61. Pagel, M. (2020). Evolutionary trees can't reveal speciation and extinction rates. Nature *580*, 461–462.

62. Nee, S., Holmes, E.C., May, R.M., and Harvey, P.H. (1994). Extinction rates can be estimated from molecular phylogenies. Philos. Trans. R. Soc. Lond. B Biol. Sci. *344*, 77–82.

63. Quental, T.B., and Marshall, C.R. (2009). Extinction during evolutionary radiations: reconciling the fossil record with molecular phylogenies. Evolution *63*, 3158–3167.

64. Freckleton, R.P., Phillimore, A.B., and Pagel, M. (2008). Relating traits to diversification: a simple test. Am. Nat. *172*, 102–115.

65. Rabosky, D.L., and Goldberg, E.E. (2017). FiSSE: A simple nonpara-metric test for the effects of a binary character on lineage diversification rates. Evolution *71*, 1432–1442.

66. Harvey, M.G., and Rabosky, D.L. (2018). Continuous traits and speciation rates: Alternatives to state-dependent diversification models. Methods Ecol. Evol. *9*, 984–993.

67. Cantalapiedra, J.L., Prado, J.L., Herna´ndez Ferna´ndez, M., and Alberdi, M.T. (2017). Decoupled ecomorphological evolution and diversification in Neogene-Quaternary horses. Science *355*, 627–630.

68. Burin, G., Alencar, L.R.V., Chang, J., Alfaro, M.E., and Quental, T.B. (2019). How Well Can We Estimate Diversity Dynamics for Clades in Diversity Decline? Syst. Biol. *68*, 47–62.

69. Kodandaramaiah, U., and Murali, G. (2018). What affects power to esti-mate speciation rate shifts? PeerJ *6*, e5495.

70. Baker, R.J., and Bradley, R.D. (2006). Speciation in mammals and the ge-netic species concept. J. Mammal. *87*, 643–662.

71. Claramunt, S., Derryberry, E.P., Remsen, J.V., Jr., and Brumfield, R.T. (2012). High dispersal ability inhibits speciation in a continental radiation of passerine birds. Proc. Biol. Sci. *279*, 1567–1574.

72. Kisel, Y., and Barraclough, T.G. (2010). Speciation has a spatial scale that depends on levels of gene flow. Am. Nat. *175*, 316–334.

73. Stanley, M.S. (1998). Macroevolution: Pattern and Process (Johns Hopkins University Press).

74. Henao Diaz, L.F., Harmon, L.J., Sugawara, M.T.C., Miller, E.T., and Pennell, M.W. (2019). Macroevolutionary diversification rates show time dependency. Proc. Natl. Acad. Sci. USA *116*, 7403–7408.

75. Simo˜es, M., Breitkreuz, L., Alvarado, M., Baca, S., Cooper, J.C., Heins, L., Herzog, K., and Lieberman, B.S. (2016). The Evolving Theory of Evolutionary Radiations. Trends Ecol. Evol. *31*, 27–34.

76. Yu, W., Xu, J., Wu, Y., and Yang, G. (2012). A comparative study of mammalian diversification pattern. Int. J. Biol. Sci. *8*, 486–497.

77. Huelsenbeck, J.P., Rannala, B., and Masly, J.P. (2000). Accommodating phylogenetic uncertainty in evolutionary studies. Science *288*, 2349–2350.

78. Moore, B.R., Chan, K.M.A., and Donoghue, M.J. (2004). Detecting Diversification Rate Variation in Supertrees. In Phylogenetic Supertrees Computational Biology, O.R.P. Bininda-Emonds, ed. (Springer Netherlands), pp. 487–533.

79. Mitchell, J.S., Etienne, R.S., and Rabosky, D.L. (2019). Inferring Diversification Rate Variation From Phylogenies With Fossils. Syst. Biol. *68*, 1–18.

80. Couzens, A.M.C., and Prideaux, G.J. (2018). Rapid Pliocene adaptive radiation of modern kangaroos. Science *362*, 72–75.

81. Brennan, I.G. (2019). Incorporating uncertainty is essential to macroecological inferences: Grass, grit, and the evolution of kangaroos. bioRxiv, 772558.

82. Steeman, M.E., Hebsgaard, M.B., Fordyce, R.E., Ho, S.Y.W., Rabosky, D.L., Nielsen, R., Rahbek, C., Glenner, H., Sørensen, M.V., and Willerslev, E. (2009). Radiation of extant cetaceans driven by restructuring of the oceans. Syst. Biol. *58*, 573–585.

83. Arbour, J.H., and Santana, S.E. (2017). A major shift in diversification rate helps explain macroevolutionary patterns in primate species diversity. Evolution *71*, 1600–1613.

84. Upham, N.S. (2014). Ecological diversification and biogeography in the Neogene: Evolution of a major lineage of American and Caribbean rodents (Caviomorpha, Octodontoidea) (University of Chicago), PhD thesis.

85. Shi, J.J., and Rabosky, D.L. (2015). Speciation dynamics during the global radiation of extant bats. Evolution *69*, 1528–1545.

86. Amador, L.I., Are´valo, R.L.M., Almeida, F.C., Catalano, S.A., and Giannini, N.P. (2018). Bat Systematics in the Light of Unconstrained Analyses of a Comprehensive Molecular Supermatrix. J. Mamm. Evol. *25*, 37–70.

87. Scornavacca, C., and Galtier, N. (2017). Incomplete Lineage Sorting in Mammalian Phylogenomics. Syst. Biol. *66*, 112–120.

88. Wagner, P.J. (2019). On the probabilities of branch durations and stratigraphic gaps in phylogenies of fossil taxa when rates of diversification and sampling vary over time. Paleobiology *45*, 30–55.

89. Smits, P.D. (2015). Expected time-invariant effects of biological traits on mammal species duration. Proc. Natl. Acad. Sci. USA *112*, 13015–13020.

90. Soul, L.C., and Friedman, M. (2015). Taxonomy and Phylogeny Can Yield Comparable Results in Comparative Paleontological Analyses. Syst. Biol. *64*, 608–620.

91. Prothero, D. (2015). Garbage in, garbage out: the effects of immature taxonomy on database compilations of North American fossil mammals. N. M. Mus. Nat. Hist. Sci. Bull. *68*, 257–264.

92. Rankin, B. (2015). Paleobiogeography of Latest Cretaceous and Early Paleocene Mammals from North America (University of Calgary), PhD thesis.

93. Eldridge, M.D.B., Beck, R.M.D., Croft, D.A., Travouillon, K.J., and Fox, B.J. (2019). An emerging consensus in the evolution, phylogeny, and systematics of marsupials and their fossil relatives (Metatheria). J. Mammal. *100*, 802–837.

94.

95. Huttenlocker, A.K., Grossnickle, D.M., Kirkland, J.I., Schultz, J.A., and Luo, Z.-X. (2018). Late-surviving stem mammal links the lowermost Cretaceous of North America and Gondwana. Nature *558*, 108–112.

95. Rabosky, D.L., Grundler, M., Anderson, C., Title, P., Shi, J.J., Brown, J.W., Huang, H., and Larson, J.G. (2014). BAMMtools: an R package for the analysis of evolutionary dynamics on phylogenetic trees. Methods Ecol. Evol. *5*, 701–707.

96. Alroy, J. (2014). Accurate and precise estimates of origination and extinction rates. Paleobiology *40*, 374–397.

97. Kocsis, A´.T., Reddin, C.J., Alroy, J., and Kiessling, W. (2019). The r package divDyn for quantifying diversity dynamics using fossil sampling data. Methods Ecol. Evol. *10*, 735–743.

98. Louca, S., and Doebeli, M. (2018). Efficient comparative phylogenetics on large trees. Bioinformatics *34*, 1053–1055.

99. Paradis, E., Claude, J., and Strimmer, K. (2004). APE: Analyses of Phylogenetics and Evolution in R language. Bioinformatics *20*, 289–290.

100. Revell, L.J. (2012). phytools: an R package for phylogenetic comparative biology (and other things). Methods Ecol. Evol. *3*, 217–223.

101. Kielan-Jaworowska, Z., Cifelli, R.L., and Luo, Z.-X. (2005). Mammals from the Age of Dinosaurs: Origins, Evolution, and Structure (Columbia University Press).

102. May, M.R., and Moore, B.R. (2016). How Well Can We Detect Lineage-Specific Diversification-Rate Shifts? A Simulation Study of Sequential AIC Methods. Syst. Biol. *65*, 1076–1084.

103. Beaulieu, J.M., and O'Meara, B.C. (2016). Detecting Hidden Diversification Shifts in Models of Trait-Dependent Speciation and Extinction. Syst. Biol. *65*, 583–601.

104. Nakagawa, S., and De Villemereuil, P. (2019). A General Method for Simultaneously Accounting for Phylogenetic and Species Sampling Uncertainty via Rubin's Rules in Comparative Analysis. Syst. Biol. *68*, 632–641.

105. Rabosky, D.L., and Lovette, I.J. (2008). Explosive evolutionary radiations: decreasing speciation or increasing extinction through time? Evolution *62*, 1866–1875.

106. Foote, M. (2000). Origination and extinction components of taxonomic diversity: general problems. Paleobiology *26*, 74–102.

107. Alroy, J. (1996). Constant extinction, constrained diversification, and uncoordinated stasis in North American mammals. Palaeogeogr. Palaeoclimatol. Palaeoecol. *127*, 285–311.

108. Alroy, J. (2008). Colloquium paper: dynamics of origination and extinction in the marine fossil record. Proc. Natl. Acad. Sci. USA *105* (*Suppl 1*), 11536–11542.

109. Alroy, J. (2015). A more precise speciation and extinction rate estimator. Paleobiology *41*, 633–639.

110. Redding, D.W., and Mooers, A.Ø. (2006). Incorporating evolutionary measures into conservation prioritization. Conserv. Biol. *20*, 1670–1678.

111. Quintero, I., and Jetz, W. (2018). Global elevational diversity and diversification of birds. Nature *555*, 246–250.

112. Steel, M., and Mooers, A. (2010). The expected length of pendant and interior edges of a Yule tree. Appl. Math. Lett. *23*, 1315–1319.

113. Sepkoski, J.J., Jr. (1998). Rates of speciation in the fossil record. Philos. Trans. R. Soc. Lond. B Biol. Sci. *353*, 315–326.

114. Jablonski, D., and Finarelli, J.A. (2009). Congruence of morphologically-defined genera with molecular phylogenies. Proc. Natl. Acad. Sci. USA *106*, 8262–8266.

STAR★METHODS

KEY RESOURCES TABLE

Reagent or resource	Source	Identifier
Deposited data		
Vertlife mammal phylogenies	[2]	http://vertlife.org/data/mammals/
Data and scripts for analyses	This paper	https://github.com/n8upham/MamDiv-fossil-vs-timetree; https://zenodo.org/record/5059100
Paleobiology Database downloaded on 16 August 2018 globally for taxon Mammalia	N/A	https://paleobiodb.org/
Expert-curated dataset from late Cretaceous–Paleocene fossil assemblages of western North America	[41]	https://royalsocietypublishing.org/action/downloadSupplement?doi=10.1098%2Frsbl.2018.0458&file=rsbl20180458supp1.xlsx
Software and algorithms		
BAMM v2.5	[28]	
BAMMtools R package	[95]	
'sqs' R function	[96]	https://bio.mq.edu.au/~jalroy/SQS-3-3.R
divDyn R package	[97]	
castor R package	[98]	
tip DR function optimized for large trees	[2]	https://github.com/n8upham/MamDiv-fossil-vs-timetree/blob/main/source_functions/tipDR_functions_correct.R
ape R package	[99]	
phytools R package	[100]	

RESOURCE AVAILABILITY

Lead contact
Further information and requests for resources and data should be directed to and will be fulfilled by the lead contact, Nathan Upham (nathan.upham@asu.edu).

Materials availability
This study did not generate new unique reagents.

Data and code availability
All data have been deposited on Github (https://github.com/n8upham/MamDiv-fossil-vs-timetree) and Zenodo (https://doi.org/10.5281/zenodo.5059100), and are publicly available as of the date of publication. All original code has been deposited at the same Github and is publicly available as of the date of publication. The DOI is also listed in the key resources table. Source data for mammal phylogenies analyzed in the paper are available at http://vertlife.org/data/mammals/. Any additional information required to reanalyze the data reported in this paper is available from the lead contact upon request.

METHOD DETAILS

Mammalian phylogeny
We conducted all analyses using the species-level mammal trees of Upham et al.[2]. Briefly, these phylogenies include 5,911 extant or recently extinct species in credible sets of 10,000 trees. They were built using a 'backbone-and-patch' framework consisting of two stages of Bayesian inference, with information from age and topological uncertainty incorporated as well as the probabilistic addition of 1,813 species that lacked DNA characters using taxonomic constraints. We analyzed the credible set of trees that was node-dated using 17 fossil calibrations.

Fossil genus durations
To assess the congruence of our extant timetree-based rate estimates with rates estimated directly from the fossil record, we analyzed

genus-level fossil occurrence data from a variety of sources. Starting from the Paleobiology Database (https://paleobiodb.org/)

downloaded on 16 August 2018 globally for taxon Mammalia, we grouped by genus after specifying the exclusion of ichnotaxa and uncertain genera, then manually cleaned the taxonomy for consistency relative to expert resources.[34,45,92–94,101] To avoid artifacts from inflated stratigraphic intervals, a known issue in public databases,[91] we merged the expert-curated dataset of Pires et al.[41] from late Cretaceous–Paleocene fossil assemblages of western North America. That interval, spanning 69.9–55 Ma, covers both the K-Pg and PETM events of interest and is thereby critical for our study. We merged 2,670 occurrences of 289 genera from Pires et al., replacing data for 193 genera from the Paleobiology Database for which genus names matched, and adding data for 96 genera that were unmatched. In total, we recovered 72,579 occurrences of 5,320 fossil genera that are allocated to crown Mammalia and younger than 131 Ma, which was our temporal cutoff point to focus analyses upon the Cretaceous-Recent (earlier Cretaceous mammal fossils are too sparsely known for the planned diversity analyses).

QUANTIFICATION AND STATISTICAL ANALYSES

Branch-specific rate shifts

We performed searches for macroevolutionary shifts using BAMM v2.5,[28] a reversible-jump algorithm for sampling birth-death rate regimes. Although extinction biases have been the focus of critiques to BAMM and related rate-shift models,[17,18,102] we note that these issues are not unique to BAMM (e.g., state-dependent models suffer similarly[16,103]), nor do they preclude the model's utility for detecting rate disjunctions in extant timetrees, regardless of their underlying cause (unsampled extinctions or a regime shift). See also Figure S4 for validation of the BAMM algorithm relative to the location of mammal tree patch clades.

We evaluated the number and location of rate shifts on 10 trees drawn randomly from the credible set, specifying globalSamplingFraction = 1.0, reflecting that the trees are taxonomically complete. Although sampling > 50 trees is generally preferred for comparative methods, computation times limited us to 10 trees for BAMM analyses, which is likely > 90% accurate (see Figure 3 in[104]), while still accounting for age and topological uncertainty. On each tree, we ran the model targeting 100 million generations, while sampling every 10,000 generations. We ran the models with settings determined using the "setBAMMpriors" function in the R package BAMMtools:[95] expectedNumberOfShifts = 1.0; lambdaInitPrior = 6.446; lambdaShiftPrior = 0.00447; and muInitPrior = 6.446. We set the model to estimate speciation rates as exponentially varying through time and extinction rates as constant (i.e., similar to an independent 'SPVAR' model within each rate regime[105]). Two of the 10 analyses finished all generations on 1 node before expiration of 168-hours of runtime (the analysis is not parallelizable) of the High Performance Computing Center at Yale University; the other 8 runs completed a mean of 46.1 million generations (range: 29.2–83.1 million) in the same time. The resultant events after a 33% burn-in (mean: 3727.4; range: 1949–6667) were then subsampled to yield 1,000 evenly spaced samples for each of 10 runs with the function "getEventData" in BAMMtools. After burn-in, all BAMM runs returned stable estimates of the log likelihood (ESS mean and range across 10 trees: 585.4, 268.9 – 1200.0; log likelihood: −15743.43, −16266.4 – −15314.5) and the total number of shift events (ESS mean and range: 827.0, 328.0–1498.0). The many nearly-equiprobable shift configurations in each tree's 95% credible set of shifts prompted us to focus on the maximum shift credibility (MSC) shift sets on a per tree basis. For the rate shifts in each MSC set, we summarized the node and clade contents implicated in the shift, and the mean net diversification rate of all branches inside the shifted clade (clade rate) versus that outside it (background rate). The ratio of clade to background rates provided the rate shift magnitude and direction, whether an increase (up shift), decrease (down shift), or a mix of both among MSC sets (labeled 'up or down').

Comparisons with fossil genus diversification

To calculate fossil diversity curves and diversification rates, we first binned fossil occurrences to 5-Ma intervals from 131–1 Ma, placing any genus that spans a given boundary in both bins. We chose a 5-Ma interval as a well-suited balance between interval length and regularity (e.g., preferred over geological stages), and ended the binning at 1 Ma rather than zero to avoid inflation from late Pleistocene fossils. This strategy also allowed us to examine bin-level diversity dynamics directly surrounding both the K-Pg event (71–66 Ma, 66–61 Ma) and PETM event (61–56 Ma, 56–61 Ma). Binning resulted in 90,548 bin-level occurrences, to which we applied shareholder quorum subsampling (SQS[96]) to ensure that uniform coverage was met for different levels of subsampling across time bins. We used quorum sizes (q) of 0.5, 0.3, and 0.1, which correspond to those proportions of frequency distribution coverage measured by Good's u on the subsampled data,[96] and performed 1,000 trials including singletons ('sqs' function available at: https://bio.mq.edu.au/ ̃jalroy/SQS-3-3.R). We estimated corresponding origination ($\mathfrak{l}$) and extinction (m) rates per time bin in the R package divDyn,[97] applying six widely used metrics: per-capita,[106,107] three-timer and corrected three-timer,[108] gap-filler,[96] and second-for-third and transformed second-for-third.[109] By comparing all six metrics, we obtained rough confidence limits for the estimation of fossil $\mathfrak{l}$ and m, which we then propagated to downstream analyses. Fossil rates were not estimable for the most recent time bin (6–1 Ma), since all metrics incorporate forward-boundary crossing.

Speciation rates

We calculated two types of speciation-rate metrics using the molecular timetree: (i) pulled speciation rates across all mammals and separately for each of 20 major clades; and (ii) tip speciation rates for each species at the present as summarized for the same 20 clades. The selected clades are monophyletic across all trees selected from the credible set of timetrees, cover nearly the full species diversity of mammals, and divide that diversity more equitably than do orders (e.g., rodents are 3 clades, bats are 2 clades). Pulled speciation rates, $\mathfrak{l}_p$, were estimated in the R package castor[98] using the function 'fit_hbd_psr_on_grid' specifying the same 5-Ma

bins interval and 10 bootstrap replicates for each of 100 mammal trees sampled randomly from the credible set. We separately calculated l_p at the instantaneous present, l_0, for each of the 20 clades using the same function in castor, also on 100 trees. Species-specific 'tip' speciation rates were estimated using the tip DR metric,[29] which is equivalent to the inverse of the equal splits measure.[29,110] This metric has been called 'DR' and 'tip-level diversification rate' (tip DR) because it approximates the expected pure-birth diversification rates for the instantaneous present,[2,111] at least when trees contain 10 or more species.[29,112] However, because tip DR is a biased estimator of birth-death net diversification when relative extinction is high (> 0.8[30]), it is best viewed as a tip-level speciation-rate metric despite the name 'tip DR', which we retain to reflect its common usage. We calculated tip DR across all 10,000 mammal trees using a large-tree optimized R function (https://github.com/n8upham/MamDiv-fossil-vs-timetree/blob/main/source_functions/tipDR_functions_correct.R). To compare these speciation-rate metrics on empirical timetrees, we plotted clade-level summaries of l_0 (median) and tip DR (harmonic mean, skewness) with 95% confidence intervals (CI) using R.

We also simulated tip DR distributions expected under a homogeneous birth-death process for comparison to those observed empirically. To do so, we first estimated clade-level l and m rates across 100 empirical subtrees for each of the 20 clades ('birthdeath' function in ape[99]), then used each set of empirical rates to simulate 1 tree of the same empirical species richness ('pbtree' function in the phytools[100]). This resulted in 20 sets of 100 simulated trees on which we then calculated tip DR values to generate expected tip DR distributions.

Fossil-correction of pulled speciation rates

Following the logic of Louca and Pennell,[20] we used the mammal fossil record for each of the 5-Ma time bins to correct or 'push' the pulled speciation rate, l_p, to the true speciation rate, l. Even though fossil genera not species were examined, using lineage-level rate information derived from fossil genus durations is an established means of inferring origination and extinction rates (e.g.,[113,114]). We used two approaches: (i) fixing the extinction rate, m, and then modeling the homogeneous birth-death (HBD) process on the timetree to estimate l; and (ii) fixing the missing fraction of extant lineages through time, $E(t)$, to estimate l. In the first approach, we used the castor function 'fit_hbd_model_on_grid' to successively set the extinction rate per time bin equal to each of the six metrics of fossil m. Only the second-for-third metric could calculate extinction for the 71-66 Ma bin, so we used that value (1.0 lineages/Ma) as fixed in all trials. We truncated the most recent 1 Ma from each of 100 mammal trees to align with the 6-1 Ma time bin, and then used each tree to estimate the HBD model. We fixed no other parameters, but set initial values for (i) the present-day sampling fraction, r_0, as 0.8 to correspond to taxonomically complete extant trees truncated at 1 Ma with an assumed speciation rate of ~0.2 species/lineage/Ma; and (ii) speciation rates per bin as the estimated fossil origination rates. Those initial values were required for the HBD model to successfully converge for all 100 trees using 10 trials.

In the second approach, we took the supplemental Equation 8 from Louca and Pennell,[20]

$$l_p = l \cdot (1 - E(t)), \tag{1}$$

where $E(t)$ is the fraction of lineages extant at age t (time before the present) that are missing from the timetree, either due to extinction or not having been sampled, and then re-arranged it to solve for speciation rate:

$$l = l_p \, '(1 - E(t)). \tag{2}$$

We determined $E(t)$ by adding the total extant lineages, as derived from the lineages through time plot for each of 100 trees ('fitted LTT' element in the output from 'fit_hbd_psr_on_grid'), to the total missing lineages, as derived from the $q = 0.3$ subsampling of fossil genus durations for each of the time bins (chosen as indicative of the general pattern of subsampled fossil richness). Those values were used to solve for pushed l at each time bin, and then compared to the pushed l values obtained using the fixed fossil extinction rates.